

Manuscript Number:

Title: Ag modified ZnS for photocatalytic water pollutants degradation:
influence of metal loading and preparation method

Article Type: Full length article

Section/Category: C. Adsorption, Catalysis and Electrochemistry

Keywords: Ag/ZnS; silver loading; UV irradiation; methylene blue; phenol

Corresponding Author: Professor Olga Sacco,

Corresponding Author's Institution:

First Author: Olga Sacco

Order of Authors: Olga Sacco; Vincenzo Vaiano; Diana Sannino; Rosaria A
Picca; Nicola Cioffi

Abstract: In this paper, the photocatalytic degradation of organic pollutants was studied using Ag/ZnS nanoparticles at different noble metal loadings. The photocatalysts were prepared using two different one step techniques (photodeposition and chemical reduction) at room temperature. Specific surface area measurement, X-ray photoelectron spectroscopy, X-ray Powder diffraction, ultraviolet-visible diffuse reflectance and Raman spectroscopy were used to analyze the prepared samples. The results revealed that Ag is present as intermediate state between nanostructured Ag₀ and Ag₂O and that the addition of silver caused a significant change of the absorption spectrum of bare ZnS, resulting in high absorbance from 400 nm to the entire visible region, due to the Ag surface plasmon band. The influence of Ag loading and preparation method was evaluated in terms of the photodegradation of methylene blue (MB) as model organic cationic dye. It was observed an enhancement of photocatalytic activity induced by silver addition in comparison to bare ZnS up to 0.1 wt% Ag loading. The results evidenced that the sample at 0.1 wt% Ag prepared by chemical reduction method presented also a higher photoactivity with respect to the sample prepared by photodeposition method at the same Ag loading (0.1 wt%). The effect of various operating parameters, such as dye concentration, photocatalyst dosage and light sources was also studied. The almost complete MB degradation was obtained by using UV-LEDs as light sources and 6 g L⁻¹ of photocatalyst dosage. Finally, the optimized Ag/ZnS photocatalyst was employed for the removal of phenol, achieving a degradation degree of 60% after 180 min of UV irradiation.

Suggested Reviewers: Giovanni Palmisano
Masdar Institute of Science and Technology
gpalmisano@masdar.ac.ae

Julie J Murcia Mesa
Universidad Pedagógica y Tecnológica de Colombia

juliejoseane@yahoo.es

Maria C Hidalgo
University of Seviglia
mchidalgo@icmse.csic.es

Giuseppina Iervolino
University of Salerno
giiervolino@unisa.it

Luigi Rizzo
University of Salerno
lrizzo@unisa.it



Dear Editor,

I kindly ask you to consider for possible publication in “**Colloid and Interface Science**”, our research paper entitled:

Ag modified ZnS for photocatalytic water pollutants degradation: influence of metal loading and preparation method

The manuscript matches the aims and scope of the journal because it is an original and novel in relation to some fields relevant for the journal. Specifically, the manuscript is focused on photocatalytic degradation of organic pollutants using Ag/ZnS nanoparticles at different noble metal loadings. For this propose, two different one step techniques (photodeposition and chemical reduction) at room temperature were employed. Specific surface area measurement, X-ray photoelectron spectroscopy, X-ray Powder diffraction, ultraviolet-visible diffuse reflectance and Raman spectroscopy were used to analyze the prepared samples. The characterizations results revealed that Ag is present as intermediate state between nanostructured Ag^0 and Ag_2O and that the addition of silver caused a significant change of the absorption spectrum of bare ZnS, resulting in high absorbance from 400 nm to the entire visible region, due to the Ag surface plasmon band. The influence of Ag loading and preparation method was evaluated in terms of the photodegradation of methylene blue (MB). The photocatalytic activity was enhancement by silver addition in comparison to bare ZnS up to 0.1 wt. % Ag loading. The effect of various operating parameters, such as dye concentration, photocatalyst dosage and light sources was also studied. The almost complete MB degradation was obtained by using UV LEDs as light sources and 6 g L^{-1} of photocatalyst dosage. Finally, the optimized Ag/ZnS photocatalyst was employed for the removal of phenol, achieving a degradation degree of 60% after 180 min of UV irradiation. The present paper has not published previously - also not in any other language- and it is not under consideration for publication elsewhere; its publication is approved by all authors.

Sincerely,

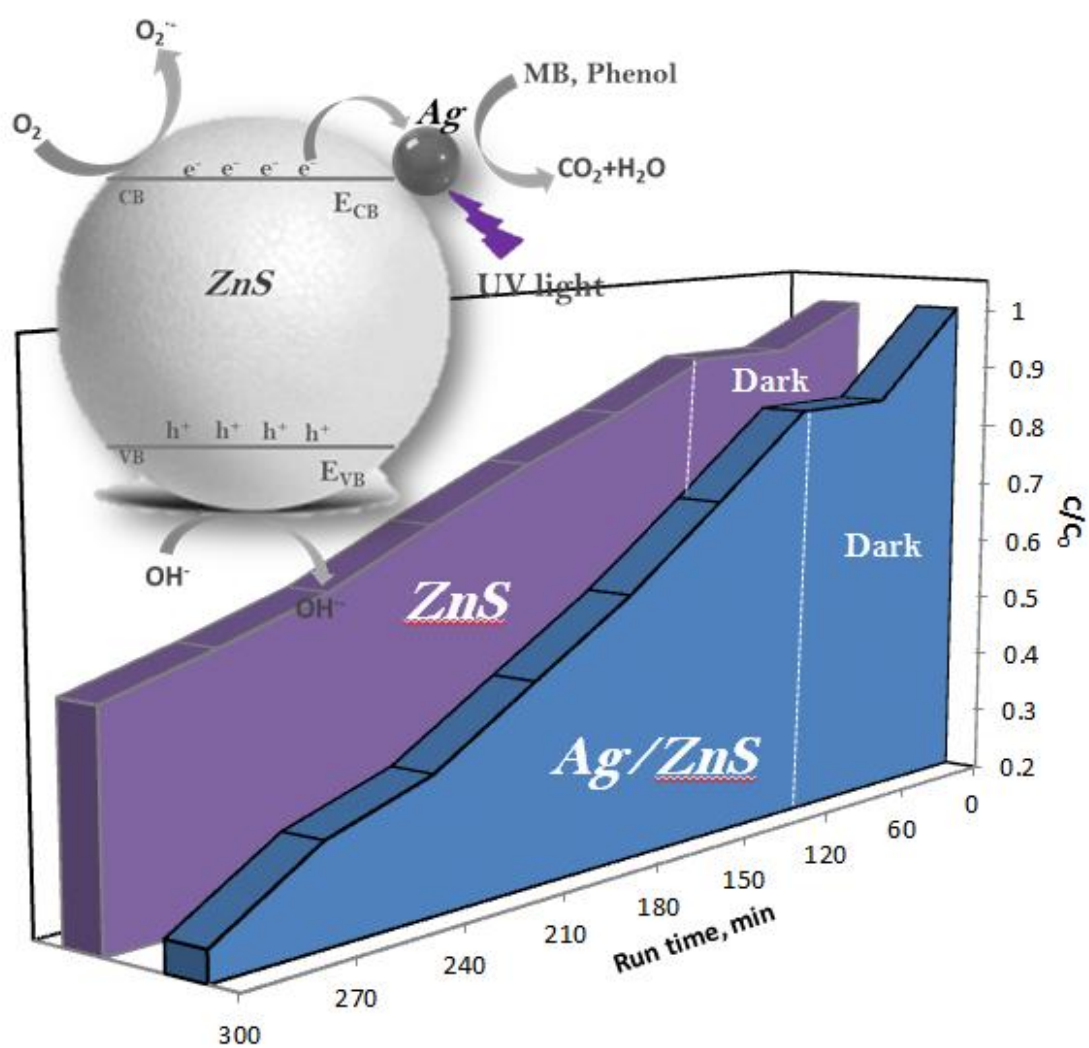
The corresponding author.

Olga Sacco, PhD

Department of Industrial Engineering

University of Salerno, Via Giovanni Paolo II 132, 84084 Fisciano (Sa), Italy

Phone (+39) 089 964006 Email: osacco@unisa.it



1
2
3
4
5
6
7
8
9
10
11
12
13
14
15
16
17
18
19
20
21
22
23
24
25
26
27
28
29
30
31
32
33
34
35
36
37
38
39
40
41
42
43
44
45
46
47
48
49
50
51
52
53
54
55
56
57
58
59
60
61
62
63
64
65

Ag modified ZnS for photocatalytic water pollutants degradation: influence of metal loading and preparation method

O. Sacco^{1*}, V. Vaiano¹, D. Sannino¹, R.A. Picca², N. Cioffi²

¹University of Salerno, Department of Industrial Engineering, Via Giovanni Paolo II

132, 84084 Fisciano (SA), Italy

²University of Bari "Aldo Moro", Department of Chemistry, Via E. Orabona 4, 70126

Bari, Italy

* Corresponding author: Tel: + 39 089 964006; E-mail: osacco@unisa.it.

Abstract

In this paper, the photocatalytic degradation of organic pollutants was studied using Ag/ZnS nanoparticles at different noble metal loadings. The photocatalysts were prepared using two different one step techniques (photodeposition and chemical reduction) at room temperature. Specific surface area measurement, X-ray photoelectron spectroscopy, X-ray Powder diffraction, ultraviolet-visible diffuse reflectance and Raman spectroscopy were used to analyze the prepared samples. The results revealed that Ag is present as intermediate state between nanostructured Ag⁰ and Ag₂O and that the addition of silver caused a significant change of the absorption spectrum of bare ZnS, resulting in high absorbance from 400 nm to the entire visible region, due to the Ag surface plasmon band. The influence of Ag loading and preparation method was evaluated in terms of the photodegradation of methylene blue (MB) as model organic cationic dye. It was observed an enhancement of photocatalytic activity induced by silver addition in comparison to bare ZnS up to 0.1 wt% Ag loading. The results evidenced that the sample at 0.1 wt% Ag prepared by chemical reduction method presented also a higher photoactivity with respect to the sample prepared by photodeposition method at the same Ag loading (0.1 wt%). The effect of various operating parameters, such as dye concentration, photocatalyst dosage and light sources was also studied.

The almost complete MB degradation was obtained by using UV-LEDs as light sources and 6 g L⁻¹ of photocatalyst dosage. Finally, the optimized Ag/ZnS photocatalyst was employed for the removal of phenol, achieving a degradation degree of 60% after 180 min of UV irradiation.

Keywords: Ag/ZnS, silver loading, UV irradiation, methylene blue, phenol

1. Introduction

Heterogeneous photocatalysis is one promising approach to protect the aquatic environment based on its ability to remove also low concentrations of organic pollutants in water [1]. In the past two decades, many oxide and sulfide semiconductors such as TiO₂, ZnO, WO₃, SrTiO₃, ZrO₂, ZnS and CdS were applied as photocatalysts for environmental control technology and also for a wide range of chemical reactions [2-4]. Among them, ZnS is an important II–VI group semiconductor existing in two main crystalline phases: α -phase (hexagonal wurtzite structure) and β -phase (cubic sphalerite structure). ZnS has been considered as a photocatalyst in different chemical reactions due to its relatively wide band gap value and the high negative value of the conduction band potential [5, 6]. In particular, the reported band gap energy of ZnS was 3.6 eV [7], meaning that it can absorb light with wavelengths below 380 nm [8]. In addition, ZnS owns additional advantages, such as good thermal stability, high electronic mobility, nontoxicity, water insolubility, and comparatively inexpensive cost [9].

When ZnS semiconductor is irradiated with photons of energy equal or greater than the band gap, an electron may be excited from the valence band into the conduction band leaving a hole in the valence band. The electron and hole can recombine and may release energy. If a suitable scavenger or surface defect is available in the semiconductor, it could trap the electron or hole and the recombination is inhibited [2]. This is a key aspect in applying ZnS as photocatalyst. In fact, for this semiconductor, the photogenerated electrons and holes easily recombine before they take part in photocatalysis [10].

Therefore, to retard the recombination of photoexcited electron–hole pairs and to enhance the photocatalysis efficiency of ZnS, one of possible approach (commonly

1 used also for other semiconductors such as TiO₂ [11, 12] and ZnO [13, 14]) is to
2 couple ZnS with materials that act as electron traps and, therefore, to extend the
3 charge carrier lifetime [15]. Numerous investigations have reported that the addition
4 of noble metals such as Au [16], Pt [17, 18] or Pd [19] enhances the overall
5 photoefficiency of photocatalysts. This effect is attributed to a reduction in the
6 recombination rate due to better charge separation between the electrons, which
7 accumulate on the metal, and the holes, which remain on the photocatalyst surface
8 [20]. Compared to the other noble metals, Ag is less expensive, so Ag based
9 photocatalysts may have a great attention to industrial practice [21-23] .

10 Many papers describe the effects of doping ZnS with silver [24-26]. In contrast, only
11 few studies report the effects of Ag deposited on ZnS nanoparticles [15]. However,
12 at our knowledge, no paper concerning the influence of Ag content on ZnS surface
13 for photocatalytic applications is present in literature.

14 Therefore, this paper reports the enhanced photocatalytic removal of organic
15 pollutants using Ag/ZnS nanoparticles at different noble metal loadings. The
16 photocatalysts were prepared using two different one step techniques
17 (photodeposition and chemical reduction). The influence of preparation method was
18 evaluated in terms of the photodegradation of methylene blue (MB) as model organic
19 cationic dye. The effect of various operating parameters, such as dye concentration,
20 photocatalyst dosage and light sources are studied. Finally, the best sample was
21 tested in the removal of phenol.

22 **2. Materials and methods**

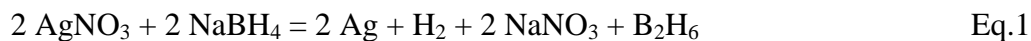
23 *2.1 Materials*

1 Zinc sulfide (ZnS), sodium borohydride (NaBH₄) and silver nitrate (AgNO₃) were
2 purchased from Sigma–Aldrich. Methylene blue (C₁₆H₁₈ClN₃S) and phenol
3 (C₆H₅OH) were purchased from Sigma–Aldrich, and used as model water pollutants
4 for photocatalytic tests.
5
6
7
8
9

10 2.2 Synthesis of Ag/ZnS nanoparticles using chemical reduction method

11 Ag/ZnS photocatalysts were synthesized through chemical reduction method starting
12 from 1 g of commercial ZnS suspended into 100 mL of distilled water. Different
13 amounts of AgNO₃ (in the range 0.785-31 mg) were added into the aqueous
14 suspension. The prepared reaction mixture was then stirred and a gaseous helium
15 flow (30 NL·h⁻¹) was bubbled inside the suspension.
16
17
18
19
20
21
22
23
24
25

26 Afterward, the reducing agent (NaBH₄) was added to the system. The added quantity
27 of NaBH₄ was calculated with respect to the amount of AgNO₃ considering the
28 stoichiometric ratio of the following reaction with an excess equal to 30%:
29
30
31
32
33
34
35



37
38
39
40
41 The suspension was left under stirring in presence of helium flow for 1 h, washed
42 with distilled water several times and finally dried overnight at room temperature.
43
44

45 The obtained Ag/ZnS photocatalysts will be denoted as xAg, where x indicates the
46 nominal Ag loading expressed as weight percentage (wt %) (Eq.4).
47
48
49
50

$$51 \quad \% \text{Ag} = \frac{g_{\text{Ag}}}{g_{\text{Ag}} + g_{\text{ZnS}}} 100 \quad \text{Eq.2}$$

52
53
54
55 Where:

56 g_{Ag} is the weight of silver calculated from AgNO₃ used in the preparation;
57
58

59 g_{ZnS} is the weight of commercial ZnS used in the preparation.
60
61
62
63
64
65

1
2
3 *2.3. Synthesis of Ag/ZnS using photodeposition method*

4 Ag/ZnS photocatalysts were synthesized through photodeposition method starting
5 from 1 g of commercial ZnS suspended into 100 mL of distilled water at room
6 temperature. 1.55 mg of AgNO₃ was then added into ZnS aqueous suspension. Then,
7 the reaction system was irradiated for 1h by two UV lamps emitting at 365 nm
8 (nominal power of 8 W, Philips). Helium (flow rate 30 NL·h⁻¹) was bubbled inside
9 the suspension during the overall irradiation time.

10
11
12
13
14
15
16
17
18
19 The photochemical reactions occurring during the photodeposition are summarized
20 as follows [18]:
21



32
33
34
35
36 After the photodeposition, the suspension was centrifuged, washed with distilled
37 water for several times and finally dried overnight at room temperature.

38
39
40 All the prepared samples are listed in Table 1.

41
42
43
44
45
46 **Table 1**

47
48
49
50 *2.4. Characterization of Ag/ZnS photocatalysts*

51
52 Different characterization techniques were used to analyze Ag/ZnS photocatalysts. In
53 particular, the specific surface area (SSA) analysis was performed by BET method
54 using N₂ adsorption with a Costech Sorptometer 1042 after a pretreatment at 35°C
55 for 2 hours in He flow (99.9990 %). X-ray photoelectron spectroscopy (XPS)
56
57
58
59
60
61
62
63
64
65

1 characterization was performed on a PHI Versaprobe II spectrometer using
2 monochromatized Al K α radiation (1486.6 eV). Both survey and high-resolution
3 (HR) spectra were acquired. Pass energy of 117.4 eV and an energy step of 1.0 eV
4 were used in the former case, whereas a pass energy of 58.7 eV and an energy step of
5 0.125 eV in the latter. C1s, O1s, Ag3d, S2p, N1s, Zn2p_{3/2}, ZnL₃M₄₅M₄₅ regions were
6 analyzed. Surface elemental composition was evaluated by MultiPack™ (v. 9.5.0,
7 PHI-ULVAC) software. Peak fitting was carried out on CasaXPS™ (v. 2.3.18).
8 Binding energy (BE) scale was corrected taking as reference the C1s aliphatic
9 component at 284.8 eV.
10

11
12 The crystalline phases of the Ag/ZnS samples were determined by X-ray Powder
13 diffraction (XRD) patterns, obtained by using a using Bruker D8 diffractometer
14 with Cu K α ($\lambda = 0.154$ nm) radiation. The diameter of the crystalline grain were
15 calculated according to Scherrer's formula [27].
16

17
18 The ultraviolet-visible diffuse reflectance spectra (UV-vis DRS) of the Ag/ZnS
19 samples were recorded using a Perkin Elmer spectrometer Lambda 35
20 spectrophotometer by means of a RSA-PE-20 reflectance spectroscopy accessory
21 (Labsphere Inc., North Sutton, NH). The optical band gap (E_{bg}) values of
22 photocatalysts were determined through the corresponding Kubelka–Munk function
23 (KM) (which is proportional to the absorption of radiation) and by plotting (KM \times
24 $h\nu$)² against $h\nu$. Raman spectroscopy studies were carried out on a Dispersive
25 MicroRaman spectrometer (Invia, Renishaw) with a laser emitting at 514 nm.
26

27 28 29 30 31 32 33 34 35 36 37 38 39 40 41 42 43 44 45 46 47 48 49 50 51 52 53 54 55 56 *2.5. Photocatalytic tests* 57 58 59 60 61 62 63 64 65

1 Methylene blue (MB) solutions were prepared by dissolving 15 mg in 1L of MilliQ-
2 grade water until to obtain an initial dye concentration equal to 15 mg L⁻¹. Phenol
3 solutions were prepared by dissolving 25 mg in 1L of MilliQ-grade water until to
4 obtain an initial phenol concentration equal to 25 mg L⁻¹.
5
6

7
8
9 The experiments were realized using a pyrex cylindrical photoreactor (ID= 2.5 cm)
10 equipped with an air distributor device ($Q_{\text{air}}=150 \text{ cm}^3 \text{ min}^{-1}$ (STP)), a magnetic stirrer
11 to maintain the photocatalyst suspended in the aqueous solution and temperature
12 controller. Four UV lamps (nominal power of 32 W, Philips) or UV-LEDs (nominal
13 power 12 W, LEDlightinghut) strips, emitting at 365 nm, were used as light sources.
14
15

16
17 The UV lamps were placed around the external surface of the photoreactor at an
18 equal distance from it (about 30 mm), while, the LEDs strip surrounded and
19 positioned in contact with the external body of the photoreactor. Prior to the
20 irradiation, the suspension was left in dark for 120 min to provide an
21 adsorption/desorption equilibrium on the photocatalyst surface and after, the
22 photocatalytic test was began under UV light irradiation up to 180 min.
23
24

25
26 During the irradiation time, slurry samples (almost 2 mL) were withdraw at fixed
27 time and then they were centrifuged to remove the catalyst powders before the
28 concentration measurement by a Perkin Elmer UV-Vis spectrophotometer at 663 nm
29 for MB concentration and at 270 nm for phenol concentration.
30
31
32
33
34
35

36 37 38 39 40 41 42 43 44 45 46 47 48 49 50 51 52 53 54 55 56 57 58 59 60 61 62 63 64 65

3. Results and Discussion

3.1 Characterization of the photocatalysts

3.1.1 Specific surface area (SSA)

Specific surface area of all sample are reported in Table 1. In particular, for Ag/ZnS

1 samples prepared by chemical reduction method, the SSA values did not change
2 significantly with respect to bare ZnS ($17 \text{ m}^2 \cdot \text{g}^{-1}$) when the Ag content was in the
3 range 0.05-0.1 wt%. With the increase of Ag content up to 4 wt%, the SSA
4 decreased to $13 \text{ m}^2 \cdot \text{g}^{-1}$, due to a possible agglomeration of the Ag nanoparticles on
5 ZnS surface, as previously observed in literature for Ag deposited on semiconductor
6 surface [28]. A similar SSA value was achieved for 0.1Ag and 0.1Ag(F) samples
7 indicating that the preparation method did not influence the textural characteristics of
8 the final samples.
9
10
11
12
13
14
15
16
17
18
19
20
21

22 *3.1.2 X-ray photoelectron spectroscopy (XPS)*

23 XPS characterization was carried out on pristine ZnS powder and on the different
24 Ag-doped samples, evaluating the surface loading of the metal as well as element
25 chemical speciation. Zn, S, and Ag (only in doped specimens) as well as C and O
26 were detected. The presence of the last two elements was expected, considering that
27 the samples were stored in air, and no sputtering treatment (e.g. with Ar^+) was
28 performed before acquiring XP spectra. Typical surface composition of all the
29 analyzed materials is reported in Table 2.
30
31
32
33
34
35
36
37
38
39
40
41
42

43 **Table 2**

44
45
46
47
48
49
50
51
52
53
54
55
56
57
58
59
60
61
62
63
64
65

Stoichiometric ratio for ZnS is preserved in all the cases. Silver surface availability tends to increase with the nominal Ag wt%, although Ag% is similar for 0.1Ag, 0.1(F)Ag, and 0.5Ag samples. This suggests that there is not a dramatic influence of the synthesis process on the dopant surface content, in agreement with other characterizations carried out in this work. Interestingly, the surface Ag wt%

1 determined by XPS is by far higher than the nominal one. This is reasonable, since
2 the nominal Ag wt% is relevant to the bulk composition, while the data calculated
3 from the XPS analyses are related to the outer nanomaterial surface. In other words,
4 silver is more present at the outer layers. Additionally, the successful reduction of
5 silver nitrate precursor and the removal of unreacted precursor (if any), upon sample
6 washing were proven since no nitrogen XP signal was detected, even on 4Ag
7 catalysts. S2p and ZnLMM signals are reported for both pristine ZnS and 0.1Ag
8 samples in Figure 1. S2p_{3/2} falls at BE = 161.6 ± 0.1 eV, characteristic of ZnS [29].
9 ZnLMM position at kinetic energy (KE) equal to 989.4 ± 0.2 eV is also compatible
10 with ZnS [29].
11
12
13
14
15
16
17
18
19
20
21
22
23
24
25
26

27 **Figure 1**

28
29
30
31 It can be seen that there is no effect on ZnS matrix (in terms of peak shift and/or
32 lineshape modification) associated to Ag doping; this holds true also at the highest
33 Ag loading (data not shown). Silver speciation was studied by investigating both
34 Ag3d and AgM₄₅N₄₅N₄₅ Auger signals [30]. Typical Ag3d region is presented in
35 Figure 2a for 0.1Ag sample; the very same region showing no peak was also reported
36 for pristine ZnS for comparison. A single doublet can be observed for 0.1Ag, whose
37 Ag3d_{5/2} component is centered at BE = 368.2 ± 0.1 eV. Peak position was unchanged
38 at other Ag loadings. Unfortunately, the chemical shift on Ag3d position associated
39 to different silver chemical environments is generally small, and their discrimination
40 is better achieved if AgMNN region is considered [30, 31]. This signal has a lower
41 intensity and was detectable only for nominal Ag wt% ≥ 2. When measurable, the
42 AgMNN spectra indicated that Ag is essentially present as slightly oxidized
43
44
45
46
47
48
49
50
51
52
53
54
55
56
57
58
59
60
61
62
63
64
65

1 nanoparticles [29]. AgMNN spectrum acquired on 4Ag sample is shown in Figure 2b.
2 The most informative position (indicated by the dotted line) falls at $KE = 356.8 \pm 0.2$
3 eV, which is attributed to an intermediate state between nanostructured Ag^0 and
4 Ag_2O . Such finding can be easily explained in terms of formation of uncapped silver
5 nanoclusters, which undergo partial oxidation upon air exposure [30].
6
7
8
9
10
11
12
13

14 **Figure 2**

15 *3.1.5 X-ray diffraction (XRD)*

16
17
18
19 The XRD patterns of bare ZnS together with the prepared Ag/ZnS photocatalysts
20 were recorded and the results are shown in Figure 3.
21
22
23
24
25
26
27
28

29 **Figure 3**

30
31
32
33 The patterns of all the samples showed a peak at about $2\theta = 28.4^\circ$, which can be
34 indexed as the (110) reflection of α -phase of ZnS (wurtzite), [32]
35 and at 28.37° , 33.19° , 47.63° , 56.49° and 76.95° , indexed respectively as (111),
36 (200), (220), (311) and (331), all assigned to β -phase of ZnS (cubic blende) [33, 34].
37
38
39
40
41
42
43

44 Because the (002) and (110) planes of the ZnS wurtzite structure overlap with the
45 (111) and (022) planes of the ZnS β -phase, the structures of both bare ZnS and
46 Ag/ZnS samples can be regarded as a mixture of ZnS α -phase and β -phase with a
47 dominant cubic sphalerite structure (β -phase).
48
49
50
51
52
53

54 No peaks for Ag are detectable for any of the Ag/ZnS samples. This is probably an
55 indication of a better dispersion and smaller metal particle size for Ag (which make it
56 undetectable with XRD technique), or to an incomplete reduction of the Ag [35, 36].
57
58
59
60
61
62
63
64
65

1 Finally, no differences in the XRD patterns of 0.1Ag and 0.1Ag(F) are observed
2 (Figure 3b).
3

4 Furthermore, the ZnS crystallite size of the samples was calculated using the
5 Sherrer's formula based on the XRD patterns and considering the diffraction peak at
6 $2\theta \sim 28.4^\circ$ (Table 1). According to these calculations, the average crystallite size of
7 bare ZnS and Ag/ZnS samples was approximately constant up to 0.1 wt% Ag content
8 and it was equal to 23nm. In addition, it is important to underline that the preparation
9 method did not induce differences in crystallites size of the sample. On the contrary,
10 by increasing the Ag amount up to 4w%, it is possible to observe also an increase of
11 crystallite size up to 26 nm. A similar behavior has been reported for Ag/ZnO and
12 Ag/TiO₂ photocatalysts [36, 37].
13
14
15
16
17
18
19
20
21
22
23
24
25
26
27
28

29 *3.1.6 UV-Vis spectroscopy (UV-vis DRS)*

30

31 The Kubelka-Munk curves, derived from reflectance spectra, of the photocatalysts
32 are shown in Figure 4.
33
34
35
36
37
38

39 **Figure 4**

40
41
42

43 Unloaded ZnS particles did not absorb light in the visible region and have an
44 absorption onset at about 360 nm with maximum absorbance at 330 nm. Compared
45 to bare ZnS, Ag/ZnS samples exhibited an increase of absorption in the UV region
46 up to 2 wt% Ag content. In details, the intensity of the main band in the range 200-
47 360 nm increased together with an increase of Ag loading from 0.05 to 0.1 wt% and
48 progressively decreased for the 0.5Ag and 2Ag samples, until to completely
49 disappear for 4Ag sample. The obtained trend is in agreement with UV-vis DRS
50
51
52
53
54
55
56
57
58
59
60
61
62
63
64
65

analysis performed on Ag-TiO₂ photocatalysts [37].

For 0.05Ag, 0.1Ag, 0.5Ag and 2Ag samples, beyond the absorption threshold of ZnS at $\lambda \leq 360$ nm, it was observed that the addition of silver caused a significant change of the absorption spectrum of bare ZnS, resulting in high absorbance from 400 nm to the entire visible region, due to the Ag surface plasmon band [38, 39]. In particular, the higher the amount of Ag content, the greater was the absorption in the visible region [15, 36]. This absorption, resulted from the presence of the Ag nanoparticles, coherently with the observation made by Yang et al. [40] regarding semiconducting materials modified with silver. A completely different absorption spectrum was achieved for 4Ag sample, evidencing only a main broad band centered at about 440 nm, due to Ag nanoparticles [41] that, probably, cover the entire ZnS surface.

The absorptions below 400 nm in the presence of silver should be attributed to the formation of silver clusters partially or totally reduced, whose stoichiometry can range from Ag₂⁺ to Ag_n^{δ+}. In particular for Ag0.1 a maximum at 337 nm, with shoulders at around 320 and 275 nm, is observed. These absorptions indicate that the charged clusters have different nuclearity. In particular, Ag₂⁺ and Ag₄²⁺ are retained to give bands at 340 and 270 nm, respectively [42]. The bands at 320 and 285 nm were typical for absorption of neutral Ag₈ and charged Ag₈⁺ clusters, respectively [43].

However, from the comparison between the spectra of Ag0.1 and Ag0.1F (figure X) the different intensity of the absorption in the range 200-400 nm may indicate a higher reduction degree of silver clusters with the NaBH₄ method since, the absorption at around 320 nm (to be attributed to neutral Ag₈ clusters) increases [44].

The E_{bg} values of the sample are reported in Table 1. The E_{bg} of bare ZnS is equal to 3.5 eV. The increase of Ag loading from 0.05 up to 0.5 wt% resulted in a slight

1 decrease of the E_{bg} that was equal to 3.4 eV for all the samples. The further increase
2 in Ag loading (2Ag and 4Ag samples) caused a reduction of the calculated E_{bg} , being
3 equal to 2.1 eV and 1.8, respectively. The observed strong decrease of E_{bg} for 2Ag
4 and 4Ag may be due to the high concentration of Ag nanoparticles on ZnS surface
5 [45]. These drastic decreases in E_{bg} can also explain the changes in UV-visible
6 absorption properties and clearly indicate a progressive metallization of samples
7 caused by the Ag [45].
8

9 These observations suggest that the amount of Ag loaded on ZnS has an important
10 effect on E_{bg} . The Mulliken electronegativity theory [46] was used for empirically
11 determine the valence band (VB) edge potential (E_{VB}) of a ground-state
12 semiconductor by using the following equation:
13
14

$$15 E_{VB} = X_{\text{Semiconductor}} - E_e + 0.5E_{bg} \quad \text{Eq.6}$$

16
17
18
19
20
21
22
23
24
25
26
27
28
29
30
31
32
33
34 Where:

35
36 $X_{\text{Semiconductor}}$ is the electronegativity of the semiconductor (in this case 5.26 eV)[47];

37
38 E_e is the energy of free electrons on the hydrogen scale (ca. 4.5 eV),

39
40
41 E_{bg} is the optical band gap energy of the semiconductor (calculated by the method
42 described above).
43

44
45
46 The conduction band CB edge potential (E_{CB}) can be determined using the following
47 relationship [48]:
48
49

$$50 E_{CB} = E_{VB} - E_{bg} \quad \text{Eq.7}$$

51
52
53
54
55
56
57
58 Because E_{bg} of bare ZnS is 3.5 eV (Table 1), the estimated E_{VB} is 2.51 eV, and the
59
60
61
62
63
64
65

1 corresponding E_{CB} is -0.99 eV. In contrast, the presence of Ag up to 0.5 wt%
2 loading determined a little variation of the E_{VB} and E_{CB} values (Table 1) meaning
3 that Ag/ZnS can maintain the strong redox potentials [49]. Ag species loaded on the
4 surface of ZnS can effectively capture the photoinduced electrons and holes. In
5 addition, the photoinduced electrons can quickly be transported to the species
6 adsorbed on the surface of ZnS under UV irradiation [50]. From the comparison
7 between 0.1Ag and 0.1Ag(F) samples, it was evidenced that, at the same Ag nominal
8 loading and using two different preparation methods, no differences in terms of E_{bg}
9 and consequently no dissimilarity in terms of E_{VB} and E_{CB} values were observed.
10 For 2Ag and 4Ag samples, the E_{bg} value was lower than the other samples and in
11 particular it was equal to 2.1 and 1.8 eV for 2Ag and 4Ag, respectively.
12
13
14
15
16
17
18
19
20
21
22
23
24
25
26
27
28

29 *3.1.7 Raman spectroscopy*

30 The Raman spectra of the samples are shown in Figure 5.
31
32
33
34
35

36 **Figure 5**

37 It is possible to observe that bare ZnS exhibited a main peak at 352 cm^{-1} , commonly
38 referred to LO mode [51, 52] of cubic blende zinc sulfide. In addition to this LO
39 peak, several weaker peaks are identified as pure acoustic or optical modes and
40 combinations of these [51-53].
41
42
43
44
45
46
47
48
49

50 After the addition of silver (Figure 5a), the intensity of the bands located at about
51 260 and 352 cm^{-1} associated to ZnS decreased and become broader up to 0.5 wt% Ag
52 loading. This phenomenon was due to alterations in the ZnS interatomic distances
53 with a surface pressure increase induced by the increase of Ag content in Ag/ZnS
54
55
56
57
58
59
60
61
62
63
64
65

1 samples [54]. For 2 and 4 wt % Ag loading, the main bands of bare ZnS tend to
2 disappear, as previously observed for Ag/TiO₂ [54].
3

4 Furthermore, the Ag deposition on ZnS surface was confirmed by the detection of
5 additional Raman bands. In particular, the signal at about 215 cm⁻¹ (whose intensity
6 increased up to 0.5 wt% Ag content) could be associated to the radial effect of Ag
7 atoms [55]. For 2Ag and 4Ag photocatalysts, the broad Raman bands approximately
8 between 380 up to about 580 cm⁻¹ are due to the presence of silver atoms producing
9 polar branches of A₁(TO) and A₁(LO) fundamental modes of Raman scattering [56]
10 Finally, the comparison between 0.1Ag and 0.1AgF evidenced that, at the same Ag
11 nominal loading, the sample prepared by chemical reduction showed a band located
12 at 215 cm⁻¹ with higher intensity than that observed for the sample prepared through
13 photodeposition method (Figure 5b).
14
15
16
17
18
19
20
21
22
23
24
25
26
27
28
29
30

31 *3.2 Photocatalytic Activity*

32 *3.2.1 Photocatalytic decolourization of MB: the influence of Ag loading on ZnS*

33
34 The photocatalytic degradation of MB under UV light irradiation using bare ZnS and
35 Ag/ZnS photocatalysts was investigated. The photocatalytic degradation was carried
36 out using 100 mL of MB solution with an initial concentration of 15 mg L⁻¹ and a
37 catalyst dosage of 3 g·L⁻¹.
38
39
40
41
42
43
44
45
46
47
48
49

50 **Figure 6**

51
52
53
54
55
56 The obtained results are reported in Figure 6. Before switching on the UV light, it
57 was evaluated the disappearance of MB due to the adsorption phenomena for 120
58
59
60
61
62
63
64
65

1 min in dark. For all Ag/ZnS samples, it is possible to observe that the presence of Ag
2 increased the MB adsorption with respect to bare ZnS. In details, MB relative
3 concentration decreased from 7% to about 14% for 0.05Ag and 0.1Ag, respectively.
4
5 For Ag loading higher than 0.1wt% (0.5Ag, 2Ag and 4Ag samples), the MB
6 concentration decrease was lower and about 11%.
7

8
9
10
11
12 After the dark period, the solution was irradiated with UV lamps and the reaction
13 started to occur. Under irradiation, the MB relative concentration progressively
14 decreased for ZnS, 0.05Ag, 0.1Ag and 0.5Ag. In particular, using bare ZnS, the MB
15 decolourization degree was equal to 45% after 180 min of UV irradiation.
16
17

18
19
20
21
22 It is worthwhile to note that, at the same irradiation time (180 min), the MB
23 decolourization increased with the increase of Ag content up 0.1wt %, while for
24 higher metal loading (0.5 wt %) the photocatalytic activity of the samples decreased
25 until to be total inhibited for 2Ag and 4Ag samples. 0.1Ag photocatalyst
26 demonstrated the highest activity among all the catalysts leading to an MB
27 decolourization equal to 55%, thus indicating that the optimal Ag content was equal
28 to 0.1wt %. The reason of this result could be attributed to the presence of Ag on
29 ZnS surface that effectively inhibits the recombination of photoinduced electron and
30 hole pairs [57]. This observation was confirmed by UV-vis DRS spectra (Figure 4) in
31 which it was evidenced the presence of plasmon band. Possibly, thanks to the
32 presence of plasmon band, a large number of photoexcited electrons were generated
33 from the Ag particles surfaces to the conduction band of ZnS and consequently the
34 photocatalytic activity increased [58].
35
36
37
38
39
40
41
42
43
44
45
46
47
48
49
50
51
52
53

54 On the other hand, the decrease of photocatalytic activity observed at higher Ag
55 content (0.5Ag) can be explained considering both that Ag particles may act as a
56 recombination center and with the increase of agglomerated Ag particles size on ZnS
57
58
59
60
61
62
63
64
65

1 (as argued from the reduction of specific surface area) surface[59]. These two effects
2 probably determined the worsening of photocatalytic activity, as also observed in
3 literature [60]. At Ag loading higher than 0.1wt%, the probability of the holes
4 capture is increased by the large number of silver particles, which decrease the
5 probability of holes reacting with adsorbed species at the ZnS surface [59]. In the
6 case of 2Ag and 4Ag, the absence of photocatalytic activity could also be explained
7 considering the UV-vis characterization. In fact, the very low optical band-gap of
8 these samples (2.1 eV for 2Ag and 1.8 eV for 4Ag) brings to the inhibition of MB
9 photodegradation process because of the possible more facile electron/hole
10 recombination in the excited state of the catalyst [15].
11
12
13
14
15
16
17
18
19
20
21
22
23
24
25
26

27 *3.2.2 Photocatalytic decolourization of MB: comparison between UV lamps and UV-* 28 *LEDs.* 29

30
31
32
33 Figure 7 show the comparison of the photocatalytic experiments carried out using
34 two different external light sources (UV lamps or UV-LEDs), at the same initial MB
35 initial concentration (15 mgL^{-1}) and 0.1Ag catalyst dosage (3 g L^{-1}).
36
37
38
39
40
41
42
43

44 **Figure 7**

45
46
47
48
49
50 The obtained values showed that, after 180 min of UV exposure time, in the case of
51 UV lamps, the MB decolourization was equal to 55% while, when UV-LEDs are
52 used as light sources, MB decolourization increased until a value of 76% was
53 reached. This last results can be explained considering that the use of the UV-LEDs
54 strip allows to reduce the dispersion of the UV photons in the external environment
55
56
57
58
59
60
61
62
63
64
65

1 due to its geometry [61] and due to higher luminous efficiency the for the LEDs that
2 consent to increase the number of photons per hour entering into reactor [61, 62].
3

4
5 *3.2.3 Photocatalytic decolourization of MB: comparison between different synthesis*
6 *method (0.1Ag and 0.1Ag(F))*
7

8 In order to compare the efficiency of Ag loaded on the ZnS prepared by different
9 synthesis method (chemical reduction and photodeposition), photocatalytic tests
10 were carried out on 0.1Ag and 0.1Ag(F) samples.
11
12
13
14
15
16
17
18
19

20 **Figure 8**
21

22
23
24
25 The decolourization of MB using the same amount of Ag loaded on ZnS surface was
26 higher for 0.1Ag than 0.1Ag(F). In particular, at the same irradiation time (Figure 8),
27 the 0.1Ag photocatalyst showed higher MB decolourization (76%) compared to
28 0.1Ag(F) (54%). Since no significant differences were observed from XPS results, it
29 is most probable for the sample 0.1Ag(F) that the decrease of adsorption (Figura 4)
30 in the UV region could be associated to the formation of Ag⁰ cluster, and therefore
31 photocatalytic activity worsened [63].
32
33
34
35
36
37
38
39
40
41
42
43
44

45 *3.2.4 Photocatalytic decolourization of MB: the influences of initial concentration*
46

47 The effect of MB initial concentration in the range 2.5-15 mg·L⁻¹, has been
48 investigated by using 0.1Ag catalyst (Figure 9).
49
50
51
52
53
54
55
56

57 **Figure 9**
58
59
60
61
62
63
64
65

1 The adsorption in dark conditions evidenced that the amount of MB adsorbed on
2 0.1Ag surface was almost constant and equal to $6.6 \pm 1.5 \text{ mg/g}_{\text{cat}}$ for all the tested MB
3 initial concentration. Under UV irradiation, at the lowest dye concentration (2.5 mg
4 L^{-1}), the MB decolourization was almost complete while was found to be reduced
5 when MB initial concentration increased up to 15 mg L^{-1} . This behavior can be
6 explained on the basis of change in optical absorption of the MB solution at varying
7 concentration [64]. The colour of solutions increased with the increase in the MB
8 concentration, limiting the penetration of the light in the aqueous medium [65]. As a
9 consequence the photocatalytic activity was lower.
10
11
12
13
14
15
16
17
18
19
20
21
22
23
24

25 *3.2.4 Photocatalytic decolourization of MB: the influences of 0.1Ag dosage*

26
27
28 The effect of 0.1Ag photocatalyst dosage (in the range $1.5\text{-}7.5 \text{ g}\cdot\text{L}^{-1}$) has been
29 investigated at 15 mg L^{-1} MB initial concentration.
30
31
32
33
34
35

36 **Figure 10**

37
38
39
40
41
42 Figure 10 shows that the photocatalytic activity increased with the increase in 0.1Ag
43 from $1.5 \text{ g}\cdot\text{L}^{-1}$ to $6 \text{ g}\cdot\text{L}^{-1}$, reaching the almost complete MB decolourization after 180
44 min of UV irradiation time. The observed enhancement in this range is probably due
45 to an increased number of available adsorption and catalytic sites on the surface of
46 0.1Ag photocatalyst [66]. When the dosage of 0.1Ag was increased up to 7.5 g L^{-1} ,
47 the decolourization rate did not change significantly. These results, commonly
48 observed for the photocatalytic slurry systems [66], can be explained considering that
49 when the photocatalyst dosage in the aqueous medium is too high, the solution
50
51
52
53
54
55
56
57
58
59
60
61
62
63
64
65

1 became turbid and the UV light were not able to penetrate and interact with the
2 photocatalyst [67]. Moreover, a possible additional explanation of the previous result
3 is that the high amount of catalyst may generate particles aggregation phenomena
4 [68] that induces the scattering of UV light, leading to worsen the photodegradation
5 efficiency.
6
7
8
9
10

11 *3.2.5 Photocatalytic degradation of phenol*

12
13
14
15
16 In order to evaluate the efficiency of 0.1Ag photocatalyst with a colorless pollutant, a
17 photocatalytic test has been carried out using an aqueous solution containing phenol.
18
19 In particular, the photocatalytic degradation of phenol under UV light irradiation
20 using bare ZnS and 0.1Ag photocatalysts was investigated Figure 11.
21
22
23
24
25
26
27
28
29
30

31 **Figure 11**

32
33
34
35
36
37 For both samples, in dark condition, the adsorption equilibrium reached the same
38 value indicating that the presence of Ag did not affect the phenol adsorption.
39
40 Different phenol degradation trend was observed under UV light. In fact using the
41 0.1Ag photocatalyst, after 180 min of UV irradiation, the degradation of phenol was
42 equal to 60% while the presence of only bare ZnS led to a phenol degradation of only
43 27%.
44
45
46
47
48
49
50
51
52
53
54
55

56 **4. Conclusions**

57
58
59 In this work the photocatalytic degradation of water pollutants under UV light
60
61
62
63
64
65

1 irradiation was studied using Ag/ZnS nanoparticles at different noble metal loadings.
2
3 The photocatalysts were prepared at room temperature using two different one step
4
5 techniques (photodeposition and chemical reduction) and they were characterized
6
7 from a chemical-physical point of view by means of different techniques. XPS
8
9 results evidenced the successful reduction of silver nitrate precursor and that Ag is
10
11 present as intermediate state between nanostructured Ag⁰ and Ag₂O. XRD analysis
12
13 showed that the structures of both bare ZnS and Ag/ZnS samples can be regarded as
14
15 a mixture of ZnS α-phase and β-phase with a dominant cubic sphalerite structure (β-
16
17 phase). Additionally, no peaks for Ag are detectable for any of the Ag/ZnS samples,
18
19 indicating a good dispersion of Ag-species. UV-Vis DRS results revealed that bare
20
21 ZnS particles did not absorb light in the visible region whereas the presence of Ag
22
23 induced an increase of absorption in the UV region up to 2 wt% Ag content.
24
25 Moreover, the addition of noble metal caused a significant change of the absorption
26
27 spectrum of bare ZnS, resulting in high absorbance from 400 nm to the entire visible
28
29 region, due to the Ag surface plasmon band. The comparison between the samples
30
31 prepared with photodeposition and chemical reduction evidenced absorption bands in
32
33 the range 200-400 nm at different intensity, indicating a higher reduction degree of
34
35 silver clusters with the chemical reduction method. Finally, the comparison between
36
37 the Raman spectra evidenced that, at the same Ag nominal loading, the sample
38
39 prepared by chemical reduction showed band located at 215 cm⁻¹ (associated to the
40
41 radial effect of Ag atoms) with higher intensity than that observed for the sample
42
43 prepared through photodeposition method.
44
45
46
47
48
49
50
51
52

53
54 The photocatalytic activity was evaluated in terms of the photodegradation of
55
56 methylene blue (MB). It was observed an enhancement of photocatalytic activity
57
58 induced by silver addition in comparison to bare ZnS up to 0.1 wt% Ag content.
59
60
61
62
63
64
65

1 The reason of this result could be attributed to the presence the presence of plasmon
2 band, able to generate large number of photoexcited electrons from the Ag particles
3 surfaces to the conduction band of ZnS. Moreover photocatalytic results evidenced
4 that the sample at 0.1 wt% Ag loading prepared by chemical reduction method
5 showed higher performances with respect to the sample prepared with
6 photodeposition method at the same Ag loading (0.1 wt%).
7
8
9
10
11
12
13

14 By using the optimized photocatalyst, the almost complete MB degradation was
15 obtained by using UV-LEDs as light sources and 6 g L⁻¹ of catalyst dosage.
16 Moreover, the optimized Ag/ZnS photocatalyst was also able to effectively degrade
17 phenol in aqueous solution under UV irradiation.
18
19
20
21
22
23
24
25
26

27 References

- 28
29 [1] S. Ameen, M.S. Akhtar, Y.S. Kim, O.-B. Yang, H.-S. Shin, *Colloid and*
30 *Polymer Science* 288 (2010) 1633.
31 [2] M.R. Hoffmann, S.T. Martin, W. Choi, D.W. Bahnemann, *Chemical Reviews*
32 95 (1995) 69.
33 [3] J. Soria, J. Sanz, M.J. Torralvo, I. Sobrados, C. Garlisi, G. Palmisano, S.
34 Çetinkaya, S. Yurdakal, V. Augugliaro, *Applied Catalysis B: Environmental* 210
35 (2017) 306.
36 [4] M. Bellardita, V. Loddo, G. Palmisano, I. Pibiri, L. Palmisano, V.
37 Augugliaro, *Applied Catalysis B: Environmental* 144 (2014) 607.
38 [5] J. Zhang, Y. Wang, J. Zhang, Z. Lin, F. Huang, J. Yu, *ACS Applied*
39 *Materials & Interfaces* 5 (2013) 1031.
40 [6] V. Vaiano, O. Sacco, D. Sannino, P. Ciambelli, *Journal of Cleaner*
41 *Production* 100 (2015) 208.
42 [7] J.N. Hart, M. Cutini, N.L. Allan, *Energy Procedia* 60 (2014) 32.
43 [8] M. Mehrabian, Z. Esteki, *Optik - International Journal for Light and Electron*
44 *Optics* 130 (2017) 1168.
45 [9] S.K. Maji, A.K. Dutta, D.N. Srivastava, P. Paul, A. Mondal, B. Adhikary,
46 *Polyhedron* 30 (2011) 2493.
47 [10] M. Jakob, H. Levanon, P.V. Kamat, *Nano Letters* 3 (2003) 353.
48 [11] E. Albiter, M.A. Valenzuela, S. Alfaro, G. Valverde-Aguilar, F.M. Martínez-
49 Pallares, *Journal of Saudi Chemical Society* 19 (2015) 563.
50 [12] M. Antoniadou, V.M. Daskalaki, N. Balis, D.I. Kondarides, C. Kordulis, P.
51 Lianos, *Applied Catalysis B: Environmental* 107 (2011) 188.
52 [13] M.-K. Lee, G. Tae, W. Kim, T. Kim, Y.-M. Sung, *Surface Plasmon*
53 *Resonance (SPR) Electron and Energy Transfer in Noble Metal– Zinc Oxide*
54 *Composite Nanocrystals*. 2008.
55
56
57
58
59
60
61
62
63
64
65

- 1 [14] K.S. Ranjith, R.B. Castillo, M. Sillanpaa, R.T. Rajendra Kumar, *Applied*
2 *Catalysis B: Environmental* 237 (2018) 128.
- 3 [15] M. Madkour, F. Al-Sagheer, Au/ZnS and Ag/ZnS nanoheterostructures as
4 regenerated nanophotocatalysts for photocatalytic degradation of organic dyes
5 References and links. 2016.
- 6 [16] A. Bumajdad, M. Madkour, Y. Abdel-Moneam, M. El-Kemary, *Journal of*
7 *Materials Science* 49 (2014) 1743.
- 8 [17] K. Saeed, I. Khan, T. Gul, M. Sadiq, *Applied Water Science* 7 (2017) 3841.
- 9 [18] V. Vaiano, M. Matarangolo, J.J. Murcia, H. Rojas, J.A. Navío, M.C. Hidalgo,
10 *Applied Catalysis B: Environmental* 225 (2018) 197.
- 11 [19] R.M. Mohamed, E.S. Baeissa, *Applied Catalysis A: General* 464-465 (2013)
12 218.
- 13 [20] S. Sato, J.M. White, *Chemical Physics Letters* 72 (1980) 83.
- 14 [21] Y.-C. Liang, C.-C. Wang, C.-C. Kei, Y.-C. Hsueh, W.-H. Cho, T.-P. Perng,
15 *The Journal of Physical Chemistry C* 115 (2011) 9498.
- 16 [22] F. Sun, X. Qiao, F. Tan, W. Wang, X. Qiu, *Journal of Materials Science* 47
17 (2012) 7262.
- 18 [23] H. Mou, C. Song, Y. Zhou, B. Zhang, D. Wang, *Applied Catalysis B:*
19 *Environmental* 221 (2018) 565.
- 20 [24] A. Sud, R.K. Sharma, INVESTIGATION OF OPTOELECTRONIC
21 PROPERTIES OF ZNS AND SILVER DOPED ZNS USING DENSITY
22 FUNCTIONAL THEORY AND CORRESPONDING DEVICE BUILD UP. 2016.
- 23 [25] E. Hao, Y. Sun, B. Yang, X. Zhang, J. Liu, J. Shen, *Journal of Colloid and*
24 *Interface Science* 204 (1998) 369.
- 25 [26] V.K. Gupta, A. Fakhri, M. Azad, S. Agarwal, *Journal of Colloid and*
26 *Interface Science* 510 (2018) 95.
- 27 [27] B.E. Warren, *X-ray Diffraction*. Dover Publications, 1990.
- 28 [28] H. Wang, X. Liu, S. Han, *CrystEngComm* 18 (2016) 1933.
- 29 [29] N.I.o.S.a. Technology, in: (Ed.)^(Eds.), Gaithersburg MD, 20899, 2012.
- 30 [30] R.A. Picca, F. Paladini, M.C. Sportelli, M. Pollini, L.C. Giannossa, C. Di
31 Franco, A. Panico, A. Mangone, A. Valentini, N. Cioffi, *ACS Biomaterials Science*
32 *& Engineering* 3 (2017) 1417.
- 33 [31] R.A. Picca, C.D. Calvano, M.J. Lo Faro, B. Fazio, S. Trusso, P.M. Ossi, F.
34 Neri, C. D'Andrea, A. Irrera, N. Cioffi, *Journal of Mass Spectrometry* 51 (2016) 849.
- 35 [32] G. Wang, B. Huang, Z. Li, Z. Lou, Z. Wang, Y. Dai, M.-H. Whangbo,
36 *Scientific Reports* 5 (2015) 8544.
- 37 [33] J.F. Xu, W. Ji, J.Y. Lin, S.H. Tang, Y.W. Du, *Appl. Phys. A: Mater. Sci.*
38 *Process.* 66 (1998) 639.
- 39 [34] M. Bodke, U. Gawai, H. Khawal, B. Dole, *Structural, Photoluminescence and*
40 *Raman spectroscopy studies on Cr substituted ZnS nanocrystals*. 2015.
- 41 [35] J. Matos, B. Llano, R. Montaña, P.S. Poon, M.C. Hidalgo, *Environmental*
42 *Science and Pollution Research* 25 (2018) 18894.
- 43 [36] C. Jaramillo-Páez, J.A. Navío, M.C. Hidalgo, *Journal of Photochemistry and*
44 *Photobiology A: Chemistry* 356 (2018) 112.
- 45 [37] S.I. Mogal, V.G. Gandhi, M. Mishra, S. Tripathi, T. Shripathi, P.A. Joshi,
46 D.O. Shah, *Industrial & Engineering Chemistry Research* 53 (2014) 5749.
- 47 [38] P. Christopher, H. Xin, S. Linic, *Nature Chemistry* 3 (2011) 467.
- 48 [39] Z. Xuming, C. Yu Lim, L. Ru-Shi, T. Din Ping, *Reports on Progress in*
49 *Physics* 76 (2013) 046401.
- 50
51
52
53
54
55
56
57
58
59
60
61
62
63
64
65

- 1 [40] D. Yang, Y. Sun, Z. Tong, Y. Tian, Y. Li, Z. Jiang, *The Journal of Physical*
2 *Chemistry C* 119 (2015) 5827.
- 3 [41] L. Gharibshahi, E. Saion, E. Gharibshahi, A.H. Shaari, K.A. Matori, E.
4 Gharibshahi, *Materials (Basel)* 10 (2017).
- 5 [42] A.N. Pestryakov, A.A. Davydov, *Journal of Electron Spectroscopy and*
6 *Related Phenomena* 74 (1995) 195.
- 7 [43] I. Tuzovskaya, N. Bogdanchikova, A. Pestryakov, V. Gurin, A. Simakov, V.
8 Lunin, *Comparison of gold and silver species supported and incorporated into*
9 *mordenites*. 2003.
- 10 [44] Y. Kotolevich, E. Kolobova, E. Khramov, J.E. Cabrera Ortega, M.H. Farías,
11 Y. Zubavichus, R. Zanella, J.D. Mota-Morales, A. Pestryakov, N. Bogdanchikova,
12 V.C. Corberán, *Molecules* 21 (2016).
- 13 [45] P. Barone, F. Stranges, M. Barberio, D. Renzelli, A. Bonanno, F. Xu, *Study*
14 *of Band Gap of Silver Nanoparticles—Titanium Dioxide Nanocomposites*. 2014.
- 15 [46] R.S. Mulliken, *The Journal of Chemical Physics* 2 (1934) 782.
- 16 [47] L.R. Hou, C.Z. Yuan, Y. Peng, *Journal of Molecular Catalysis A: Chemical*
17 *252* (2006) 132.
- 18 [48] C. Xu, Y. Liu, B. Huang, H. Li, X. Qin, X. Zhang, Y. Dai, *Applied Surface*
19 *Science* 257 (2011) 8732.
- 20 [49] L. Yuan, B. Weng, J.C. Colmenares, Y. Sun, Y.-J. Xu, *Small* 13 (2017)
21 1702253.
- 22 [50] Y. Zhou, G. Chen, Y. Yu, Y. Feng, Y. Zheng, F. He, Z. Han, *Physical*
23 *Chemistry Chemical Physics* 17 (2015) 1870.
- 24 [51] S. Kim, T. Kim, M. Kang, S.K. Kwak, T.W. Yoo, L.S. Park, I. Yang, S.
25 Hwang, J.E. Lee, S.K. Kim, S.-W. Kim, *Journal of the American Chemical Society*
26 134 (2012) 3804.
- 27 [52] A.V. Baranov, Y.P. Rakovich, J.F. Donegan, T.S. Perova, R.A. Moore, D.V.
28 Talapin, A.L. Rogach, Y. Masumoto, I. Nabiev, *Physical Review B* 68 (2003)
29 165306.
- 30 [53] h. Linfeng, M. Chen, W. Shan, T. Zhan, M. Liao, X. Fang, X. Hu, L. Wu,
31 *Stacking-Order-Dependent Optoelectronic Properties of Bilayer Nanofilm*
32 *Photodetectors Made From Hollow ZnS and ZnO Microspheres*. 2012.
- 33 [54] Z.V. Quinones-Jurado, M.A. Waldo-Mendoza, H.M. Aguilera-Bandin, E.G.
34 Villabona-Leal, E. Cervantes-Gonzalez, E. Perez, *Mater. Sci. Appl.* 5 (2014) 895.
- 35 [55] M. Buşilă, V. Musat, T. Textor, V. Badilita, B. Mahltig, *Photocatalytic and*
36 *antimicrobial Ag/ZnO nanocomposites for functionalization of textile fabrics*. 2014.
- 37 [56] S. Adhikari, A. Banerjee, N.K. Eswar, D. Sarkar, G. Madras, *RSC Advances*
38 5 (2015) 51067.
- 39 [57] J. Liqiang, W. Dejun, W. Baiqi, L. Shudan, X. Baifu, F. Honggang, S.
40 Jiazhong, *Journal of Molecular Catalysis A: Chemical* 244 (2006) 193.
- 41 [58] B. Sarma, B.K. Sarma, *Applied Surface Science* 410 (2017) 557.
- 42 [59] D.-S. Lee, Y.-W. Chen, *Journal of the Taiwan Institute of Chemical*
43 *Engineers* 45 (2014) 705.
- 44 [60] C. Sahoo, A.K. Gupta, *Journal of Environmental Science and Health, Part A*
45 50 (2015) 1333.
- 46 [61] V. Vaiano, O. Sacco, M. Stoller, A. Chianese, P. Ciambelli, D. Sannino,
47 *International Journal of Chemical Reactor Engineering* 12 (2014).
- 48 [62] K. Davididou, C. McRitchie, M. Antonopoulou, I. Konstantinou, E.
49 Chatzisyneon, *Journal of Chemical Technology & Biotechnology* 93 (2018) 269.
- 50 [63] N.D. Cvjeticanin, N.A. Petranovic, *Zeolites* 14 (1994) 35.
- 51
52
53
54
55
56
57
58
59
60
61
62
63
64
65

- [64] L.B. Reutergårdh, M. Iangphasuk, *Chemosphere* 35 (1997) 585.
- [65] V. Vaiano, M. Matarangolo, O. Sacco, D. Sannino, *Applied Catalysis B: Environmental* 209 (2017) 621.
- [66] U.G. Akpan, B.H. Hameed, *Journal of Hazardous Materials* 170 (2009) 520.
- [67] C. Zhu, L. Wang, L. Kong, X. Yang, L. Wang, S. Zheng, F. Chen, M. Feng, Z. Huang, *Chemosphere* 41 (2000) 303.
- [68] V. Vaiano, O. Sacco, D. Sannino, W. Navarra, C. Daniel, V. Venditto, *Journal of Photochemistry and Photobiology A: Chemistry* 336 (2017) 191.

1
2
3
4
5
6
7
8
9
10
11
12
13
14
15
16
17
18
19
20
21
22
23
24
25
26
27
28
29
30
31
32
33
34
35
36
37
38
39
40
41
42
43
44
45
46
47
48
49
50
51
52
53
54
55
56
57
58
59
60
61
62
63
64
65

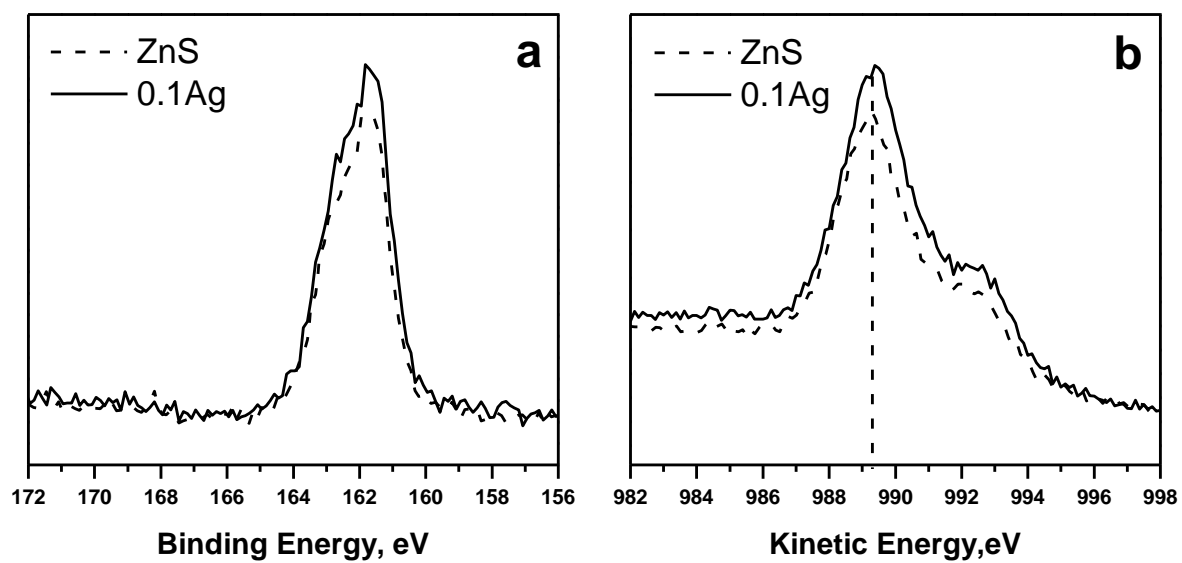


Figure 1 (a) S2p and (b) ZnLMM spectra relevant to bare ZnS (dashed curves) and to 0.1Ag sample (solid curves)

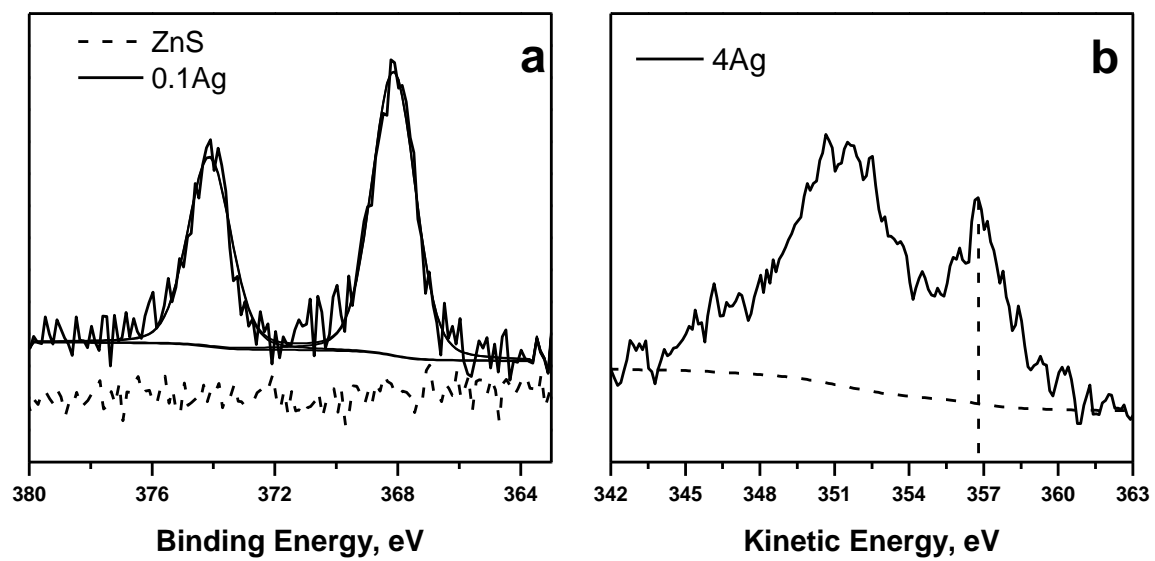


Figure 2 (a) Ag3d spectra relevant to bare ZnS (dashed curves) and to 0.1Ag (solid curves). Curve-fit of Ag3d doublet is shown; (b) AgMNN region associated to 4Ag. Auger peak position is indicated by the vertical dotted line.

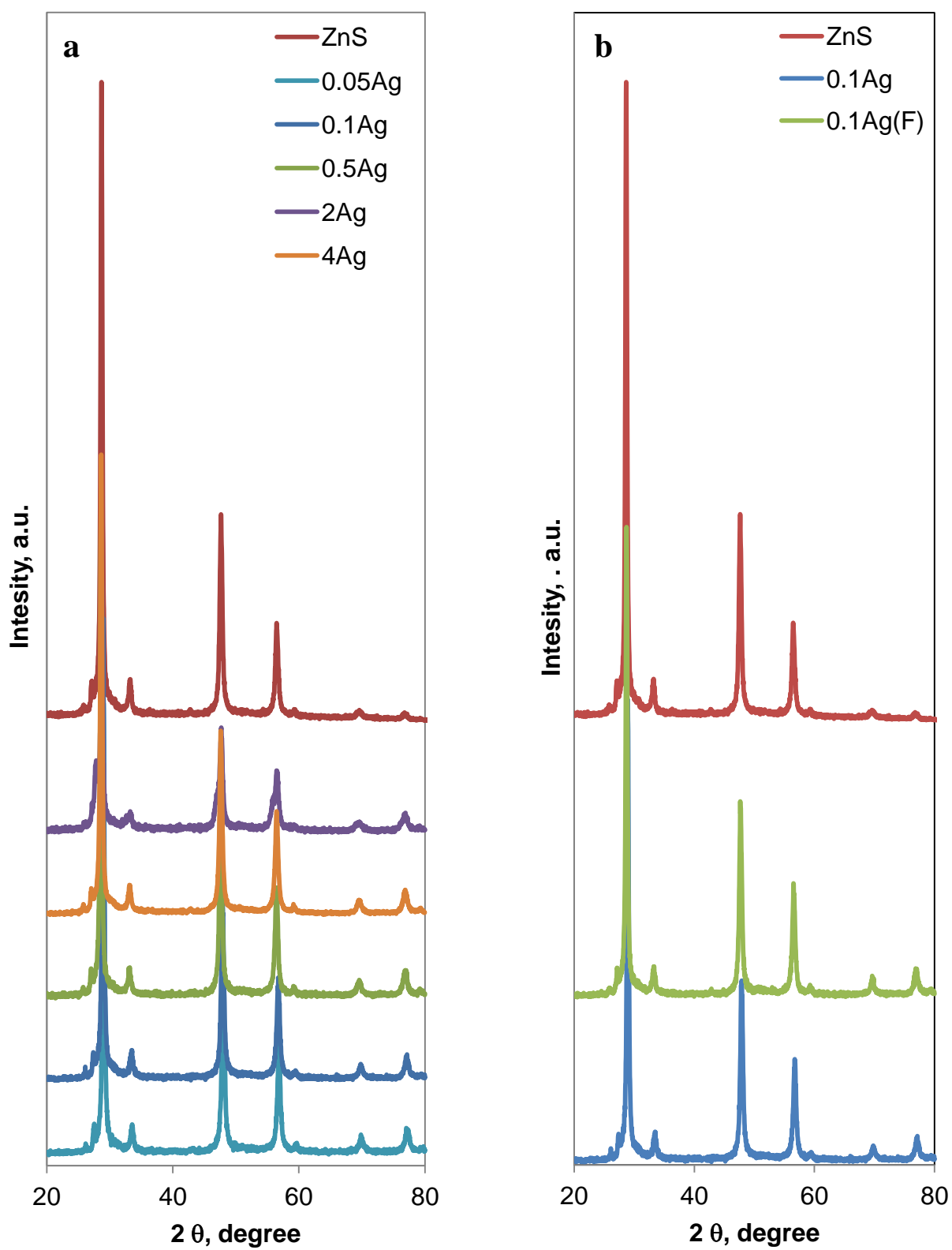


Figure 3 XRD patterns of (a) ZnS and Ag/ZnS samples and (b) ZnS, 0.1Ag and 0.1Ag(F)

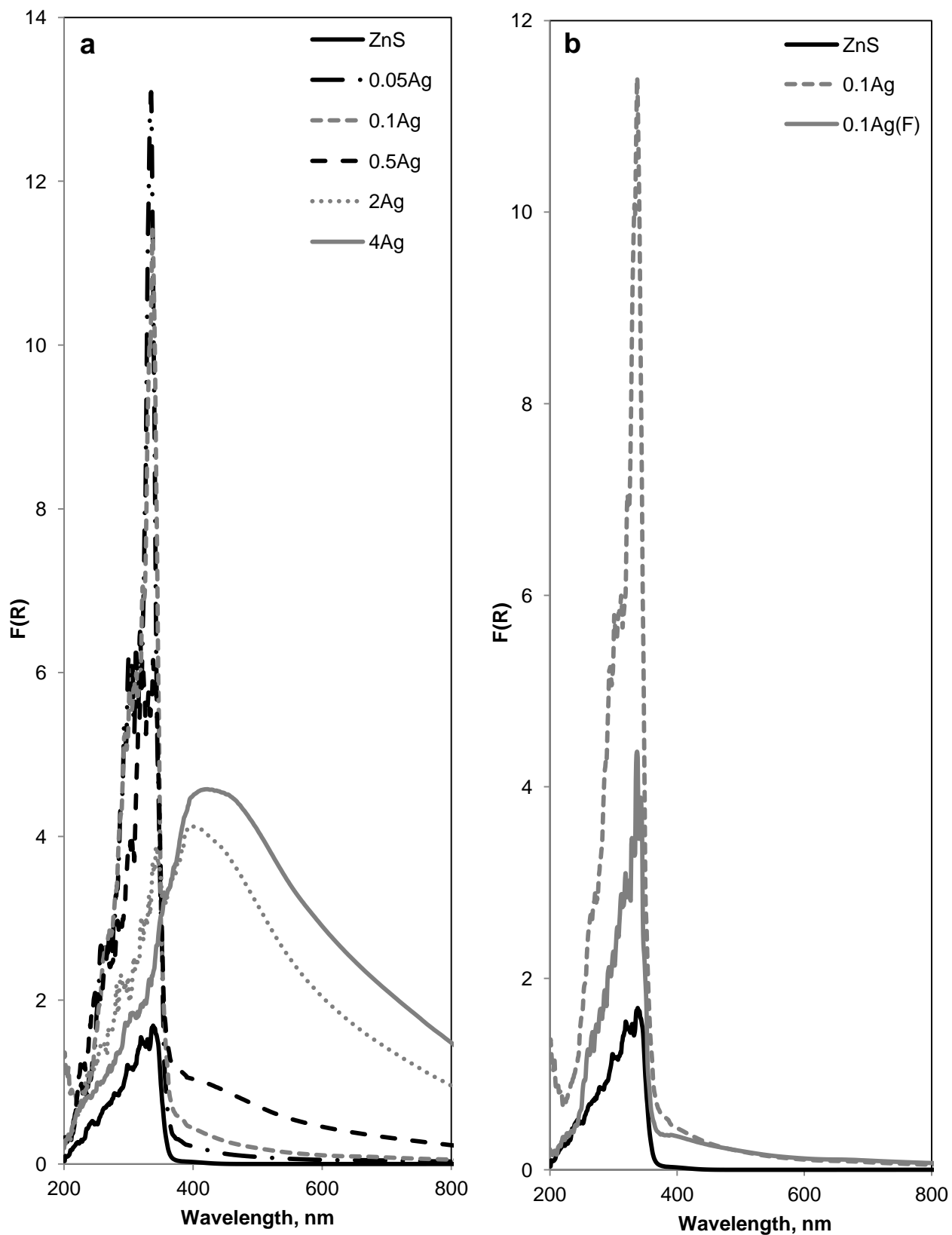


Figure 4 Kubelka Munk from UV-Vis spectra in the range 200-800nm for (a) bare ZnS and Ag/ZnS samples; (b) bare ZnS, 0.1Ag and 0.1Ag(F) samples

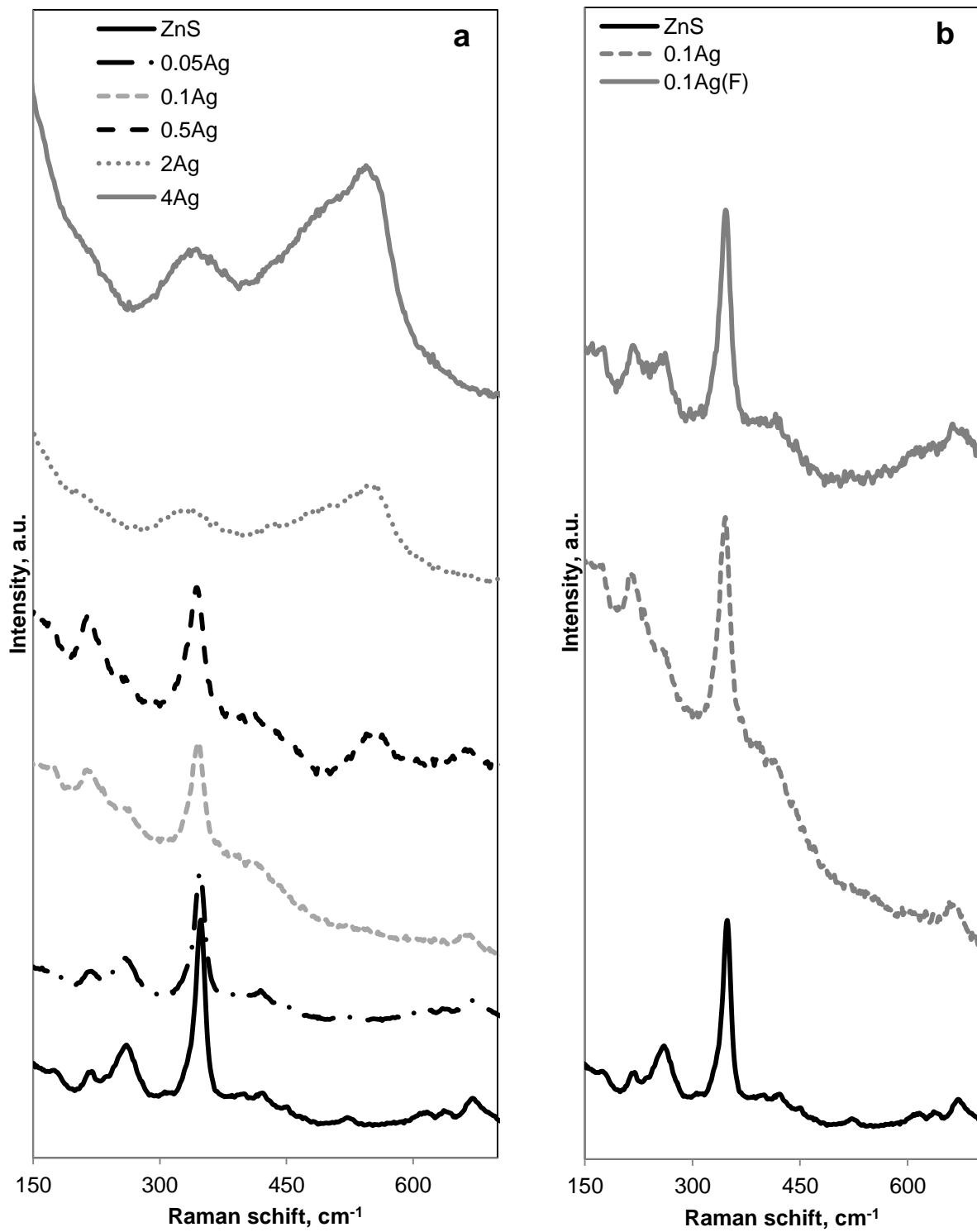


Figure 5 Raman spectra of (a) bare ZnS and Ag/ZnS samples and (b) bare ZnS, 0.1Ag, 0.1Ag(F)

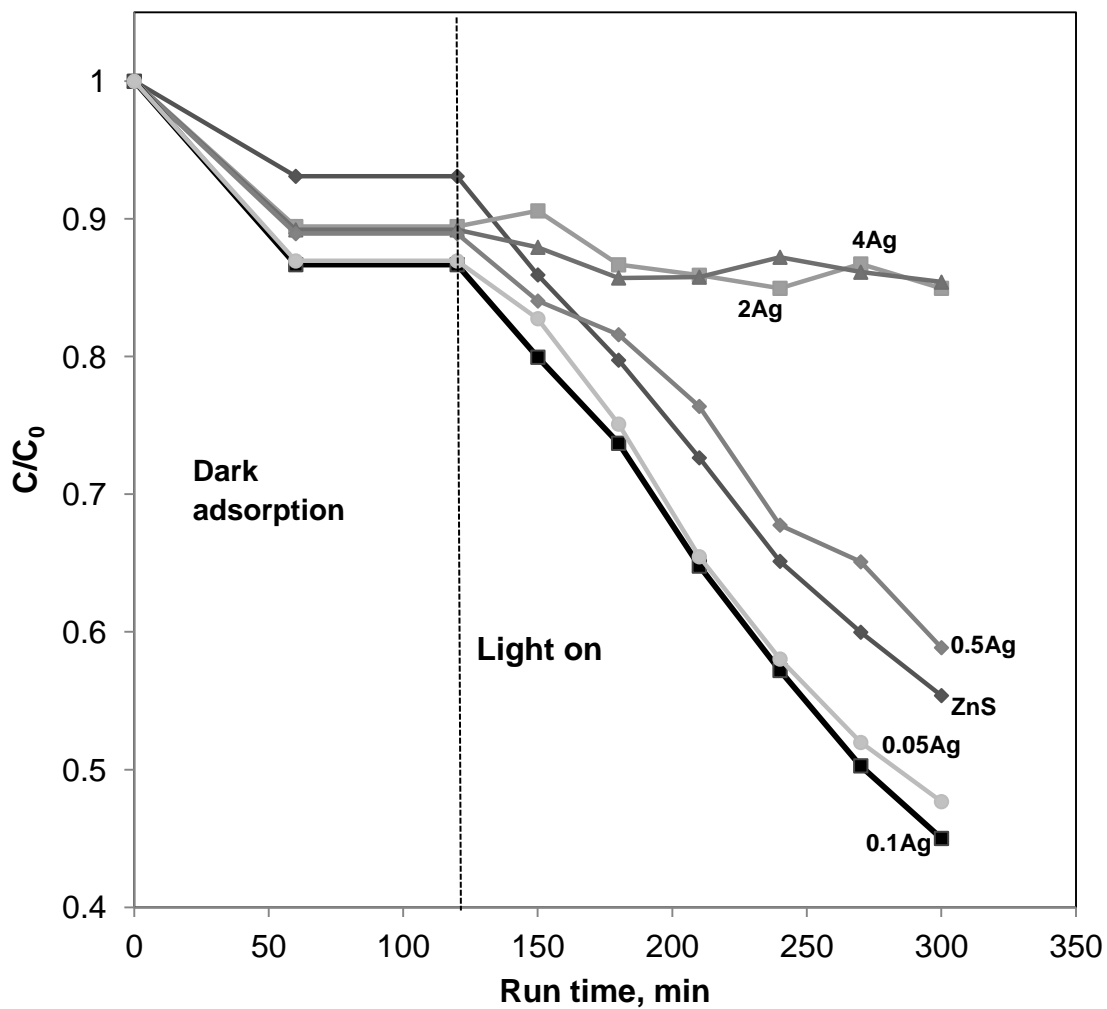


Figure 6 Photocatalytic MB decolourization over bare ZnS and Ag/ZnS catalysts; MB initial concentration: 15 mg L^{-1} ; solution volume: 100 ml ; photocatalyst dosage: 3 g L^{-1} ; light sources: UV lamps

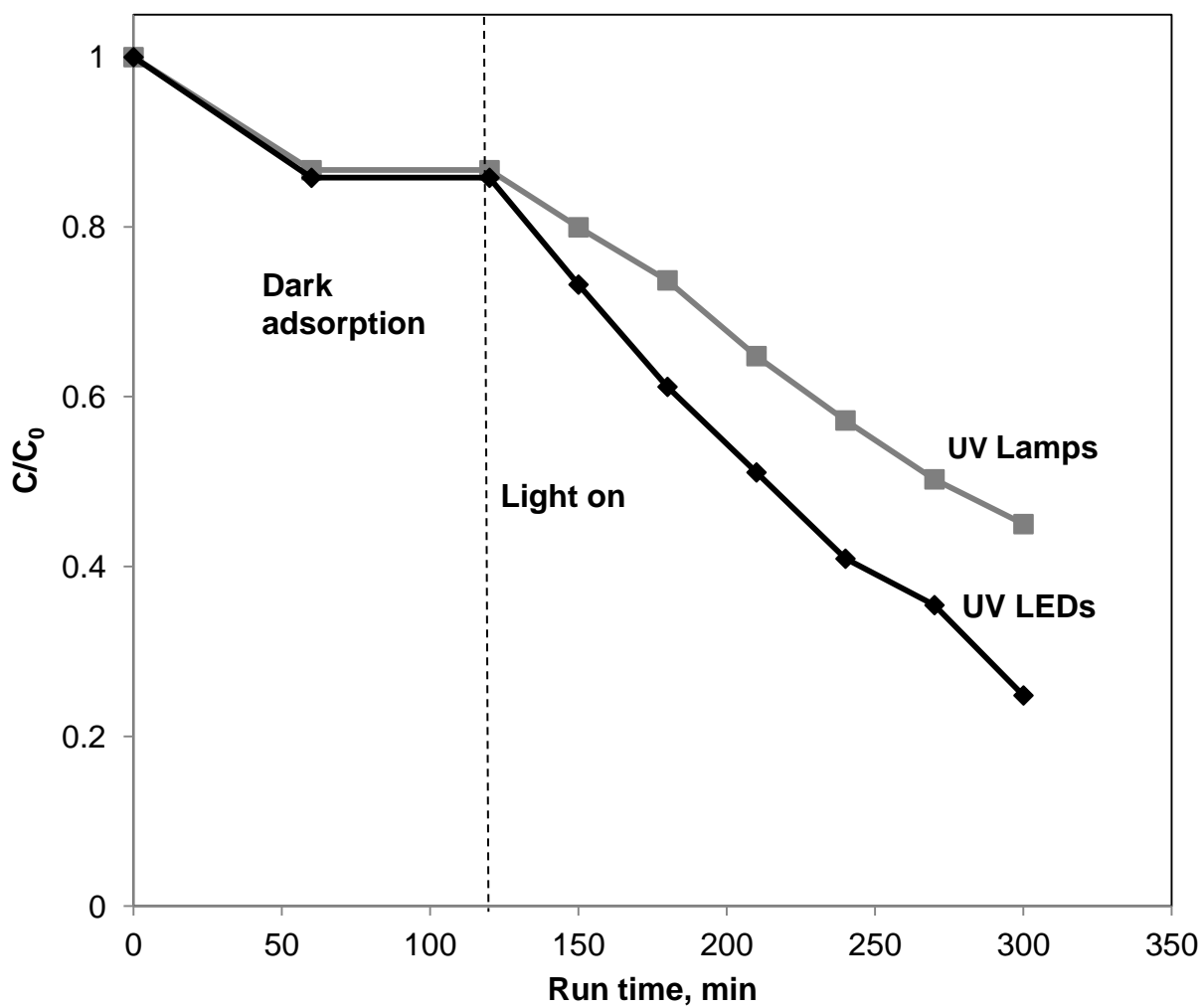


Figure 7 Photocatalytic decolourization of MB in the presence of UV-LEDs and UV-lamps 0.1Ag photocatalyst; MB initial concentration: 15 mg L^{-1} ; solution volume: 100 ml; photocatalyst dosage: 3 g L^{-1}

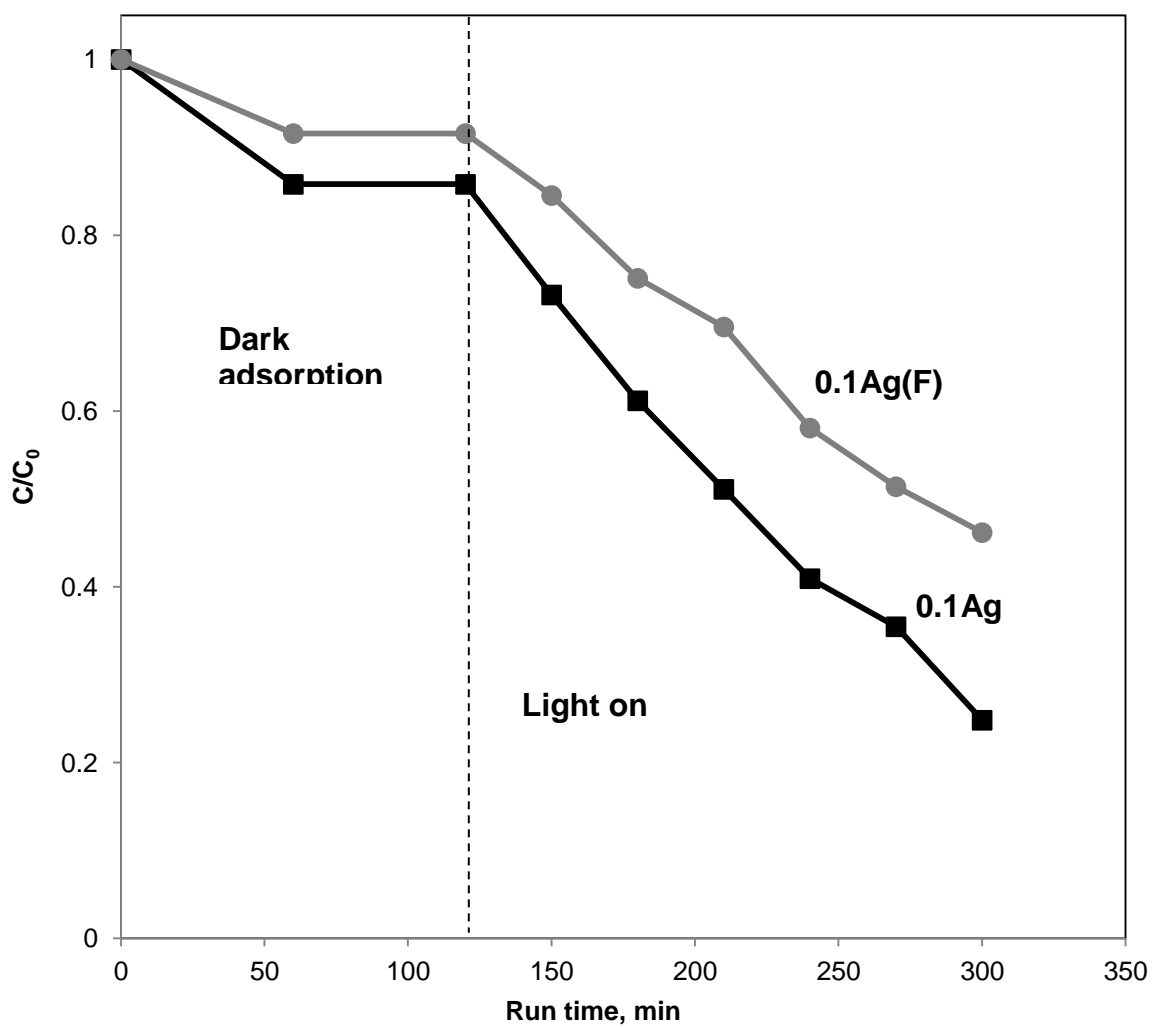


Figure 8 Photocatalytic MB decolourization under UV light (LEDs) over 0.1Ag and 0.1Ag(F) catalysts; MB initial concentration: 15 mg L^{-1} ; solution volume: 100 ml; photocatalyst dosage: 0.3 g L^{-1}

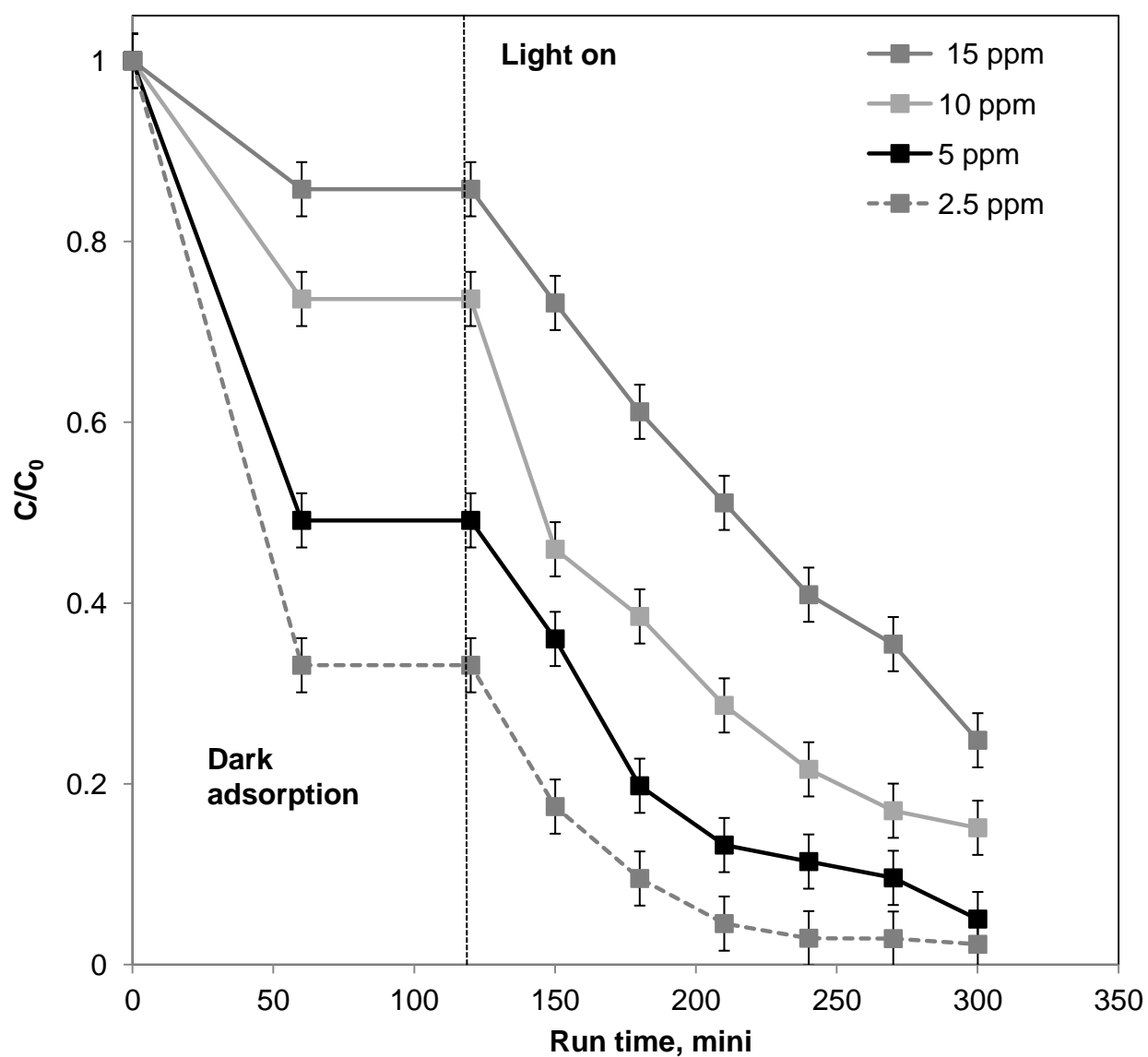


Figure 9 Influences of MB initial concentration; photocatalyst: 0.1Ag; solution volume: 100 ml; photocatalyst dosage: 0.3g L⁻¹; light sources: UV LEDs

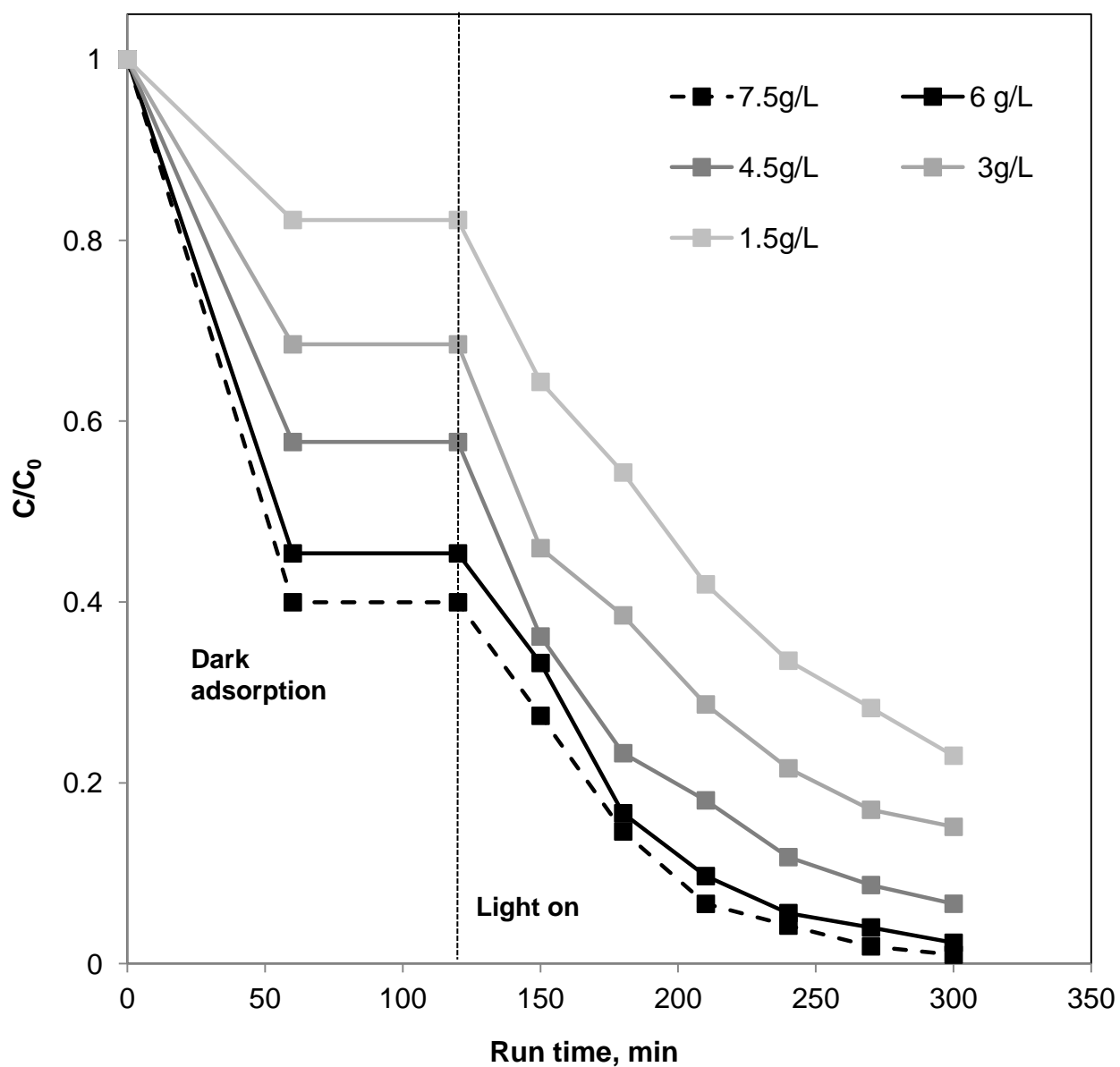


Figure : Influences of photocatalyst (0.1Ag) amount; initial concentration: 15 mg L^{-1} ; solution volume: 100 ml; light sources: UV LEDs

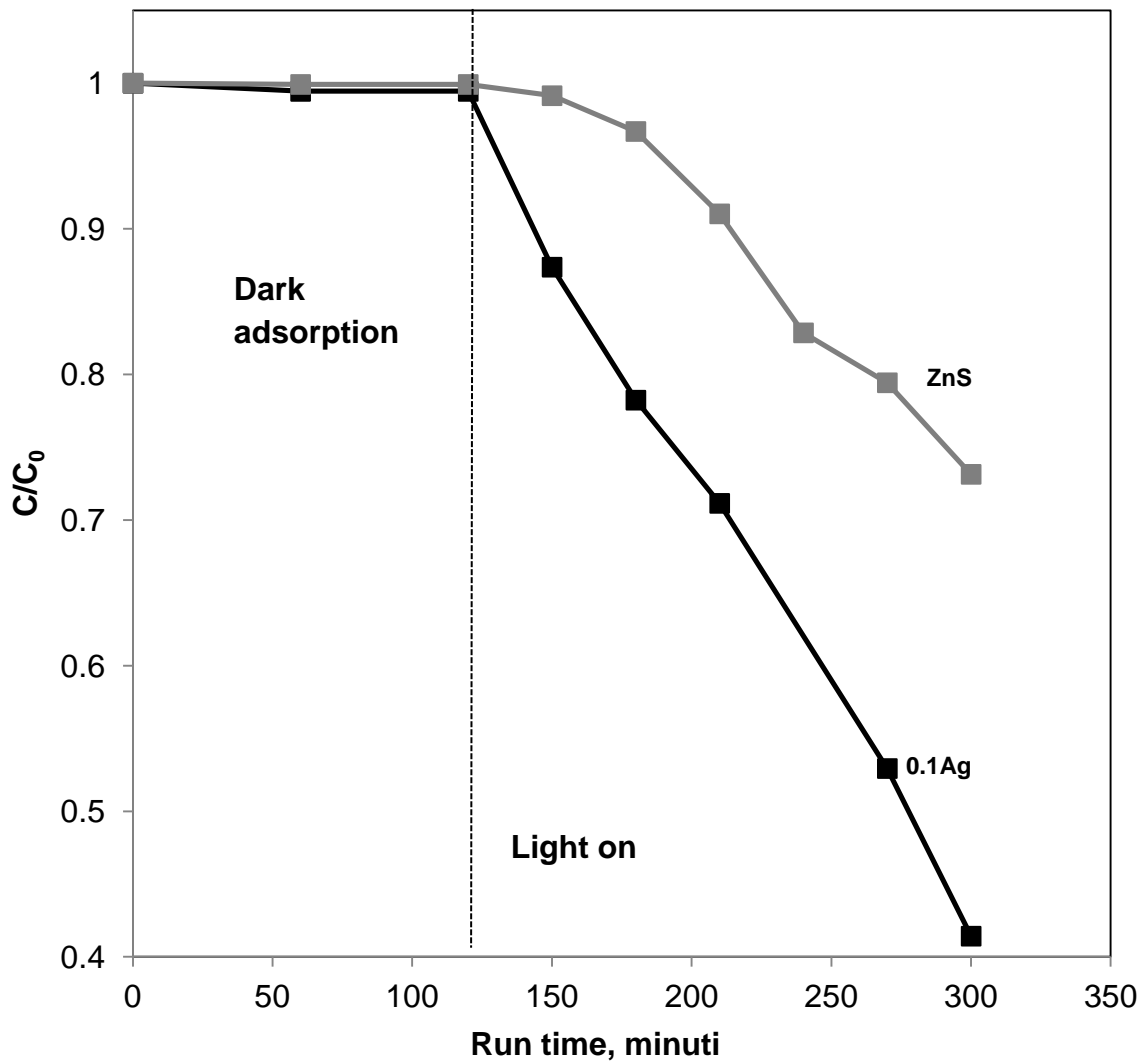


Figure 11 Photocatalytic degradation of phenol over bare ZnS and 0.1Ag catalysts; phenol initial concentration: 25 mg L^{-1} ; solution volume: 100 ml; photocatalyst dosage: 0.3 g L^{-1} ; light sources: UV LEDs

Table 1 Ag nominal loading, crystallites size, specific surface area (SSA), band- gap energy (E_{bg}), valence band edge potential (E_{VB}) and conduction band CB edge potential (E_{CB})

Catalyst	Nominal loading Ag, wt%	Crystallite size, nm	SSA, m ² /g	E_{bg} , eV	E_{VB} , eV	E_{CB} , eV
ZnS	-	22	17	3.5	3.075	-1.555
0.05Ag	0.05	23	16	3.4	2.51	-0.99
0.1Ag	0.1	23	16	3.3	2.46	-0.94
0.1Ag (F)	0.1	22	17	3.4	2.41	-0.89
0.5Ag	0.5	24	15	2.8	2.46	-0.94
2Ag	2	25	14	2.1	2.16	-0.64
4Ag	4	26	13	1.8	1.81	-0.29

Table 2 Surface chemical composition of bare ZnS and Ag/ZnS for different Ag wt% loadings (error on atomic percentages (At%) is $\pm 0.2\%$ for Ag and Zn, and $\pm 0.5\%$ for the other elements). The surface silver weight % calculated from XPS data (Ag wt %) is reported in the last column.

Sample	Zn%	S%	Ag%	C%	O%	Ag wt %
ZnS	16.6	17.8	-	54.4	11.2	-
0.05Ag	30.3	28.9	0.6	29.0	11.2	1.8
0.1Ag	32.0	31.1	1.4	26.3	9.2	4.1
0.1Ag(F)	32.8	31.0	1.3	26.0	8.9	3.8
0.5Ag	31.6	30.1	1.3	27.3	10.5	3.8
2Ag	21.8	21.9	2.4	43.4	10.5	8.4
4Ag	22.9	21.1	5.7	37.3	13.0	17.8